Within- and across-genus scaling of vessel diameter reveals consistent hydraulic responses to rainfall

Elijah Magistrado[1*], Isaac Towers[1], Jugo Ilic[1], Zoe Ball[1], and Daniel Falster[1]

[1]Evolution and Ecology Research Centre, University of New South Wales Sydney, NSW 2052, Australia

*Corresponding author: e.magistrado@student.unsw.edu.au

Summary

- Xylem vessel diameter and lumen fraction are expected to track water availability via the hydraulic safety–efficiency trade-off yet observed trait–rainfall relationships are weak and inconsistent. This discrepancy may partly reflect the conflation of within- and across-lineage effects in comparative datasets.
- We tested this possibility by analysing hydraulically weighted vessel diameter (Dh) and vessel lumen fraction (VLF) across 480 Australian native species from 129 genera. Using linear mixed-effects models with genus-level centering, we partitioned trait–climate relationships into within- and across-genus components along a precipitation gradient, comparing results to a conventional linear model.
- D_h scaled positively with mean annual precipitation (MAP) at both within- and across-genus levels, with similar slopes but differing intercepts among lineages. The centering model explained 11.0% of variance from MAP alone and 78.6% including taxonomic effects, versus 2.8% for the conventional model. VLF showed no significant climate relationship, with variation associated mainly with phylogenetic grouping.
- Separating within- and across-group responses offers a possible explanation for inconsistencies reported in vessel size–climate scaling: vessel size tends to increase with rainfall, while much of the remaining variance may relate to differing baseline hydraulic strategies across lineages, reflected as intercept differences. Within-subject centering is underused in plant ecology and could help reduce ecological fallacies in phylogenetically diverse studies.

Key words: vessel diameter, vessel lumen fraction, mean annual precipitation, wood anatomy, climate scaling, within-subject centering

Introduction

The hydraulic traits of plants vary systematically across climatic gradients, shaped by the opposing selective pressures of maximising water transport capacity and avoiding drought-induced embolism. The hydraulic safety-efficiency trade-off predicts that species in wetter environments should favour higher xylem conductivity, investing in vessel anatomy that maximises water transport capacity at the cost of greater vulnerability to drought-induced embolism. Conversely, species in drier environments should favour safer, lower-conductivity xylem that resists cavitation under more negative water potentials (Tyree & Ewers, 1991; Sperry *et al.*, 2008; Pfautsch *et al.*, 2016). These predictions have been attributed to commonly observed hydraulic outcomes: embolism resistance scales with mean annual precipitation globally (Choat *et al.*, 2012), and eco-evolutionary optimality models predict that sapwood conductivity should decline as soils dry, as the costs of embolism risk outweigh the photosynthetic benefits of higher water transport rates (Towers *et al.*, 2024). Vessel size and vessel lumen fraction (VLF), the proportion of the cross-sectional area of the stem occupied by vessel lumen, are among the most mechanistically direct contributors to conductivity. Larger vessels provide disproportionately large increases in conductivity at the risk of higher hydraulic failure (Tyree & Zimmermann, 2002), while higher VLF allows for more conducting area at the cost of reducing the available space for non-lumen functions such as parenchyma and fibre tracheids (Zanne *et al.*, 2010). Consequently, these traits should vary with rainfall, with wider vessels and higher VLF favoured in wetter environments where hydraulic demand is greater and cavitation cost lower (Carlquist, 1977; Tyree & Zimmermann, 2002; Pfautsch *et al.*, 2016; Towers *et al.*, 2024).

Despite strong theoretical expectations, the relationship between vessel size and rainfall is inconsistent across studies and often weaker than relationships involving other hydraulic traits. Several studies report only weak vessel size responses to substantial aridity gradients (Cornwell & Ackerly, 2009; Martínez-Cabrera *et al.*, 2009; Morris *et al.*, 2018; Liu *et al.*, 2019; Zheng *et al.*, 2019; Peters *et al.*, 2021), whereas outcomes such as predawn water potential, turgor loss point, and hydraulic conductance respond more reliably (Choat *et al.*, 2012; Peters *et al.*, 2021). Vessel size also responds to temperature, particularly across freezing boundaries due to the impacts of freeze-induced embolisms (Zanne *et al.*, 2014; Morris *et al.*, 2018). Some have also argued that any apparent aridity signal reflects vessel tapering and height-climate covariation rather than a direct hydraulic response (Olson *et al.*, 2014; Fajardo *et al.*, 2020). Collectively, these findings call into question the role of vessel size in plant responses to aridity, prompting a stronger focus on more direct measures of hydraulic behaviour such as P50 (Choat *et al.*, 2012; Gleason *et al.*, 2016; Liu *et al.*, 2019).

However, studies that focus on one or a few genera have consistently found stronger responses of vessel diameter to rainfall (Schreiber *et al.*, 2015; Pfautsch *et al.*, 2016; Bourne *et al.*, 2017), compared to larger, more diverse samples (Morris *et al.*, 2018; Peters *et al.*, 2021; Wang *et al.*, 2025), suggesting the relationship may be phylogenetically structured. For example, Bourne et al. (2017) and Pfautsch et al. (2016) each demonstrated a strong positive relationship between the vessel sizes to rainfall within species of *Eucalyptus*. This suggests an intriguing possibility that differences in hydraulic strategies across evolutionary lineages may manifest themselves as differences in intercepts and/or slopes, which blur the relationship of vessel size to climate in phylogenetically diverse studies (Fig. 1). If true, any study

failing to account for these differences would report a weak or non-significant relationship where a strong one exists.

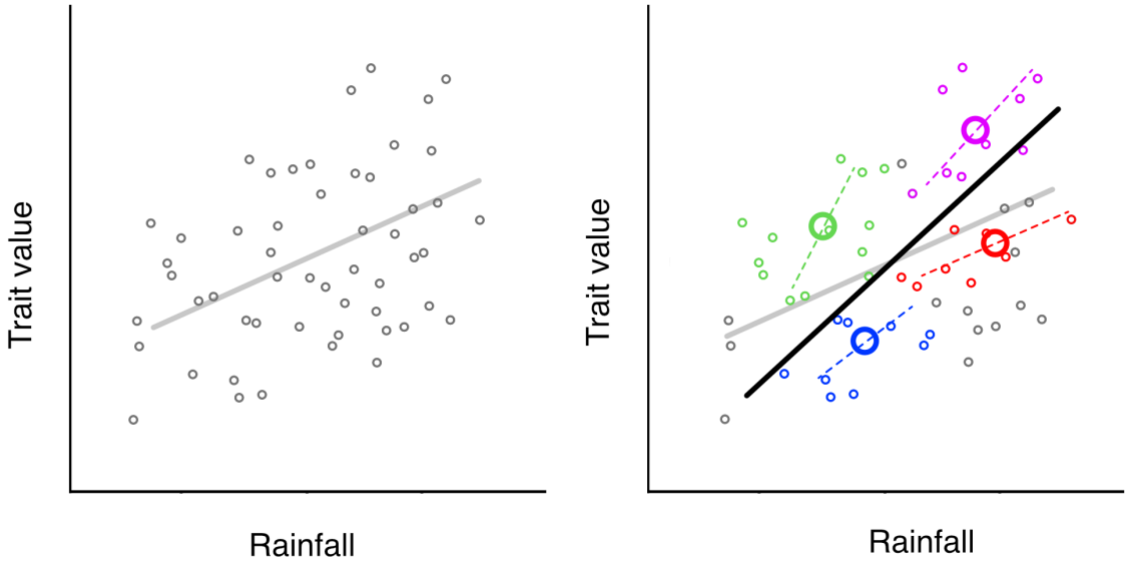

Fig. 1 A conceptual figure showing the difference between a simple linear regression model (left) and a within-subject centering model (right). Within-subject centering reveals the differences in slopes and intercepts across different groups within the same set of data (black line) compared to only using the overall data (grey line). It also visualises the differences in slope and intercept across different groups (coloured dots and lines, mean values in larger circle) which are disregarded in a simple linear regression.

A similar argument can be made for responses of VLF to rainfall or aridity. Theoretically, we might expect VLF to increase with rainfall to enhance hydraulic conductivity and growth where water is abundant (Gleason *et al.*, 2013). Additionally, a high VLF may also increase vessel connectivity and facilitate embolism spread, resulting in drier environments favouring lower VLF (Avila *et al.*, 2023). However, a high VLF with a high density of smaller vessels may have advantages by providing redundancy of alternative pathways for water flow around cavitated vessels (Tyree & Zimmermann, 2002). Empirical studies show mixed evidence, with some finding a positive relationship (Cornwell & Ackerly, 2009; Gleason *et al.*, 2012) and others not (Dong *et al.*, 2022). But again, differences between major plant groups may blur the

relationship. Indeed, several authors have reported strong differences between major taxa (genera, families) in the average VLF (Zheng *et al.*, 2019).

There are strong theoretical reasons to expect lineage-specific differences in both the intercept and slope of vessel trait–rainfall relationships. Hydraulic outcomes are inevitably influenced by multiple factors beyond water availability alone: vessel size and lumen fraction interact with wood density, vessel grouping, pit membrane properties, and the balance between conducting and non-conducting tissue, all of which vary among lineages and may shift the baseline level of conductivity independently of rainfall (Zanne *et al.*, 2010; Barotto *et al.*, 2016; Choat *et al.*, 2018; Levionnois *et al.*, 2021; Mrad *et al.*, 2021). Where a lineage has evolved a particular anatomical strategy — dense wood, grouped vessels, or high tracheid investment, for example — this will interact with the general vessel size response to water availability, producing differences in intercept even where the direction of the rainfall relationship is conserved. Stearns (1992) argues that such lineage-specific effects are a general feature of trait evolution: traits adapt to climate, but also to one another, such that the same selective pressure can produce different anatomical solutions in different groups. The cross-sections in Figure 2 illustrate this directly, showing notable differences in vessel arrangement, size distribution, and tissue composition across taxa exposed to similar climatic conditions. We therefore expect the physical relationship between vessel anatomy and conductivity to be expressed differently across lineages, not because the underlying hydraulics differ, but because the anatomical context in which vessels operate does.

In principle, accounting for differences in intercept or slope among major taxa is straightforward. By fitting an appropriate statistical model, we can both test for the

127 separation of the responses within and across taxonomic groups and simultaneously
128 reveal stronger effects of specific traits. For example, Isasa et al. (2023) found that
129 separating responses within and across species revealed the interspecific relationship
130 of D_h to P50 that was otherwise not seen in pooled data. Yet, most large-scale studies
131 use simpler linear models that pool all variation (Gleason *et al.*, 2016; Zanne *et al.*,
132 2018; Morris *et al.*, 2018; Liu *et al.*, 2019; Peters *et al.*, 2021), thus disregarding the
133 potential differences in response within and between each higher-level phylogenetic
134 group. In this context, it is not surprising that studies focusing on one genus reveal
135 stronger patterns, as they are effectively isolating variation from other factors.

136 Large-scale testing of lineage-specific anatomical strategies has long been
137 constrained by the labour-intensive nature of microscopic analysis and the
138 methodological heterogeneity of compiled trait databases. Vessel anatomy requires
139 microscopic analysis of stem cross-sections, and studies using consistent
140 methodology across large numbers of species are rare. Most direct measurements
141 are confined to small sample sizes — typically single genera or a handful of co-
142 occurring species — making it difficult to separate the effects of water availability from
143 those of phylogeny, tree size, or local environmental variation (Pfautsch *et al.*, 2016;
144 Peters *et al.*, 2021). Large-scale analyses of vessel traits have instead relied on data
145 accumulated across diverse sources and methodologies (Zanne *et al.*, 2010; Morris
146 *et al.*, 2018; Liu *et al.*, 2019), which introduces considerable variation in sampling
147 protocols, stem position, and trait definitions. Few studies have examined vessel size
148 and lumen fraction across more than 100 species using consistent methods, leaving
149 the generality of the predicted rainfall relationships poorly tested.

Here, we use historical wood collections to assemble a large, phylogenetically diverse dataset to overcome some of the sampling constraints limiting previous work. Although historical specimens often lack precise georeferencing, these collections allow for large-scale analyses of anatomical measurements across a wide climate range at a scale not achievable through direct field sampling. We use this dataset to test how vessel size and VLF vary with rainfall across a broad range of taxa, and whether accounting for phylogenetic structure resolves the inconsistent relationships reported in the literature. We hypothesise that (1) vessel diameter and VLF increase with rainfall overall; (2) separating the within- and across-group effects would account for a large portion of the variance in the trait-climate relationships, improving model fit over conventional linear models; (3) and that the direction and magnitude of within-genus responses will diverge, reflecting lineage-specific anatomical strategies.

Materials and Methods

Dataset and sampling

Source material comprised historical stained wood slides curated by the Forestry Corporation of New South Wales and accessed through the National Herbarium of New South Wales at the Australian Botanic Gardens Mount Annan. The sampled dataset encompasses 480 native Australian species across 129 genera and 32 families. The wood collection was created primarily for the purposes of species identification of timber, some samples as early as the 1920s. The samples were taken from near the base of the trees, on the outer heartwood near the sapwood boundary for consistency in wood construction. The arrangement of vessels, fibre, and parenchyma are distinct across lineages which allow for relatively easy identification to the genus level (Fig. 2).

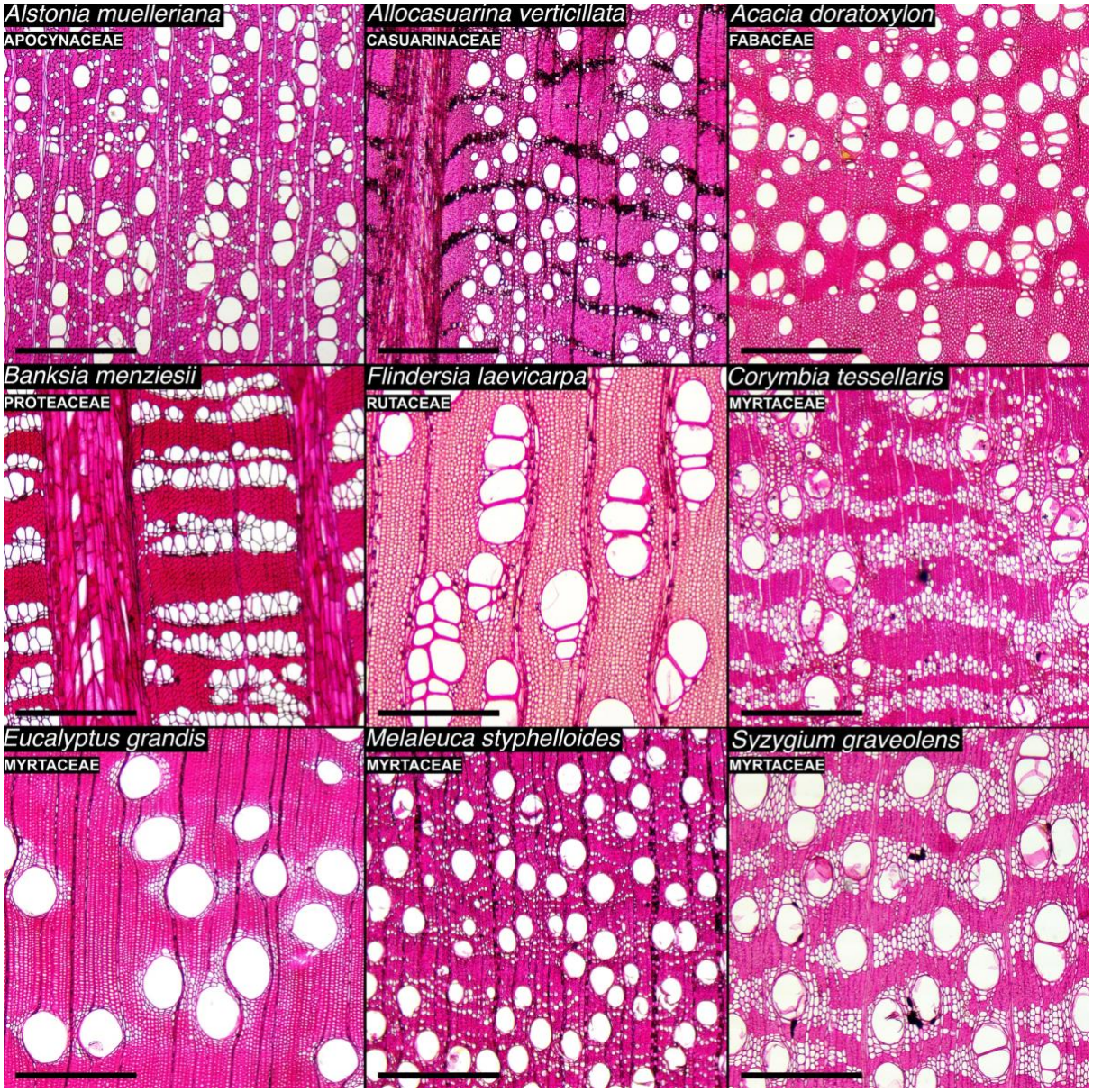

Fig. 2 Differences in wood anatomy across different genera and families. *Corymbia*, *Eucalyptus*, *Melaleuca*, and *Syzygium* species have notable differences in wood anatomy despite all being part of the Myrtaceae family. Scale bars are 500 μm.

The source material and the sampled species are biased towards canopy species considered for use in forestry, such as *Eucalyptus* (Table 1). However, the sample remains largely representative of the Australian woody vegetation since Australia's forests are dominated by eucalypt (i.e., *Eucalyptus*, *Corymbia*, and *Angophora* species) and *Acacia* species (ABARES, 2023), and the sampled species cover a large proportion of the climate niches occupied by Australian native species (Fig. 3).

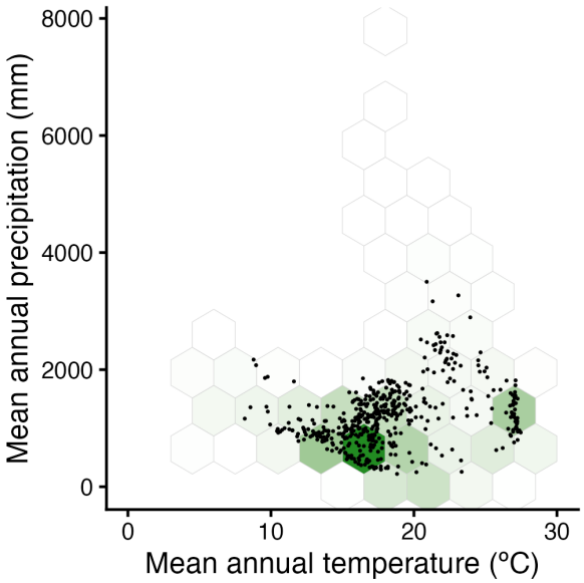

Fig. 3 Climate distribution of all tracheophytes species in Australia (darker green represents more species). The overlaid black points are the study species (n = 480).

Table 1 The dataset has a heavy sampling bias towards species of interest to forestry, clearly shown by the top 5 most sampled genera representing 47% of total sample diversity.

	Number of species	% of total
Myrtaceae	**221**	**46**
Eucalyptus	131	27
Corymbia	21	4
Syzygium	17	4
Melaleuca	14	3
Other Myrtaceae	38	8
Fabaceae	**56**	**12**
Acacia	44	9
Other Fabaceae	12	3
Remaining species	**203**	**42**

Each wood slide was marked with the species name and a unique tree code and typically had two images available. The images selected were for Australian native species collected in Australia only. Images were excluded if the wood sample itself had excessive damage due to improper sample handling (i.e., large tears) that significantly altered the geometry of the vessel lumen. Images with poor image quality (i.e., blurry,

low contrast) were included if the vessels were distinct and undamaged, as the image processing step allowed for accurate measurements.

The APCalign R package (Wenk *et al.*, 2024) was used to update the species names to the latest accepted taxonomy and to confirm native status according to the Australian Plant Census (APC) and the Australian Plant Name Index (APNI). APC is the standard taxonomy endorsed by the Council of Heads of Australasian Herbaria (CHAH) where taxonomy is agreed upon by major Australasian herbaria. APNI is the index that documents and lists the plant names and references present in the APC.

Image processing

The historical wood collection was available as digitised images. The images were digitally cleaned due to visual artefacts from the digitisation and from the wood slides themselves (Fig. S1). Brightness, contrast, and white balance were corrected to ensure the vessel lumen were as clear and distinct as possible. Changes to the size of the vessel lumen were minimised to prevent misleading measurements. Vessels were selected by cropping a vertical section of the image, prioritising undamaged sections of the sample. All images used the same scale with 4x magnification and ~0.9905 mm per pixel. This meant that species with smaller vessels typically had significantly more vessels measured per image. On average, there were three images per species, and approximately 80 vessels measured per image. The mean vessel area was calculated per species by averaging all measured vessels for that species across all images.

The vessels were measured primarily using a semi-automated script in the image analysis software QuPath v0.6.0 (Bankhead *et al.*, 2017). The process is based on

image segmentation and pixel thresholding as the lumen area of the vessels are distinctly brighter in colour and much larger in size than the non-vessel lumen parts of the image. The process is mostly automated, with the script initially highlighting most of the vessel lumen correctly. However, manual checks were conducted per image to ensure the lumen areas were selected correctly. The script highlights areas that are large enough to be considered a vessel, but this varies across different taxa and samples.

Anatomical measurements

The vessel size measurement used is the hydraulically weighted diameter (D_h) which accounts for the disproportionately large increase in conductivity for a relatively small increase in diameter, according to the Hagen-Poiseuille Law. This approach has been used in many studies (Peters *et al.*, 2021; Isasa *et al.*, 2023). It is calculated as the function (Equation 1) adapted from Sperry and Saliendra (1994):

$$D_h = \frac{\sum d^5}{\sum d^4}. \quad (1)$$

The diameter, *d* is derived from the area measurements of each vessel, *A*, assuming the shape of the vessel to be circular (Equation 2):

$$d = 2 \times \sqrt{\frac{A}{\pi}}. \quad (2)$$

The measurements of the vessel areas were verified by comparing the data to the measurements from Zanne et al. (2010). For the D_h analyses, only full vessels (Fig. S1, green lines) were used. The part vessels (Fig. S1, blue lines) were used for the

VLF analyses where the part vessel areas still count towards the total vessel lumen area.

Vessel lumen fraction (VLF) was used as a proxy for vessel connectivity, as used in Avila et al. (2023). It is calculated as the sum of all vessel areas (including part vessels) divided by the total area of the image multiplied by a hundred (Equation 3):

$$\mathrm{VLF} = \frac{\sum A_{\mathrm{vessel}}}{A_{\mathrm{image}}} \times 100. \quad (3)$$

Species climate distribution

Since the samples were not precisely georeferenced, it was not possible to create sample-level climate data. Instead, species-level climate data were created by using GBIF occurrence data (GBIF.org, 2026) and historical MAP data (1970-2000) from WorldClim 2.1 (Fick & Hijmans, 2017). Climate data using occurrence data have been used by other studies as a method of representing a species' entire range (Morris *et al.*, 2016) and have evidence of being a reliable proxy (Bourne *et al.*, 2017).

The GBIF data was filtered to only include observations after 1900, inside Australia, and only tracheophytes to limit the processing power and file sizes required to create the climate preference tables. Only occurrence data with a coordinate accuracy of 1,000 m or less and marked as human observations were used to match the spatial resolution of the climate rasters. Only species with 10 or more occurrence records were used to exclude species with limited information. The climate variable selected for the analyses was mean annual precipitation (MAP) as it is the most common representation of climate in similar studies. The values for MAP for each observation were extracted from the 30 seconds resolution (i.e., one pixel represents roughly 1 km

261 x 1 km) WorldClim 2.1 raster files and averaged for each species to represent its
262 climate preference.

263 Statistical analyses

264 All statistical analyses were conducted in R v4.5.3 (R Core Team, 2026) using the
265 *easystats* v0.7.5 (Lüdecke *et al.*, 2022), *glmmTMB* v1.1.14 (Brooks *et al.*, 2017), and
266 *tidyverse* v2.0.0 (Wickham *et al.*, 2019) packages. All analyses were conducted on
267 species-level mean trait values by averaging all measurements across all images for
268 a species. Taxonomic grouping was used as the main indicator for phylogenetic
269 structure. This approach has limitations, with taxonomy ever-changing. However, our
270 analyses found conserved wood anatomical traits within genera (Fig. 2) which likely
271 reflect shared evolutionary lineages.

272 To separate within- and across-genus responses, we fitted a linear mixed-effects
273 model with genus-level centering (Equation 4). This approach partitioned the data into
274 two distinct responses to rainfall: the across-genus effect (i.e., the variation in mean
275 trait values across genera) and the within-genus effect (i.e., the variation among
276 species within a single genus) as previously demonstrated in Figure 1:

277 $$y_{ijk} = \beta_0 + \beta_{\text{across}}\bar{x}_j + \beta_{\text{within}}\left(x_{ijk} - \bar{x}_j\right) + u_{0k} + u_{0j} + u_{1j}\left(x_{ijk} - \bar{x}_j\right) + \varepsilon_{ijk}. \quad (4)$$

278 This model represents the trait value (either D_h or VLF) as y_{ijk} and MAP as x_{ijk} for
279 species *i* in genus *j* and family *k*. The predictor variable x_{ijk} has been separated into
280 two components, $\bar{x}_j$ for the genus-level mean MAP and $x_{ijk} - \bar{x}_j$ for the species-level
281 mean MAP deviation from the genus-level mean MAP. This notation explicitly
282 separates the across-genus (b_{across}) and within-genus (b_{within}) slopes. u_{0k} and u_{0j}

represent the variable intercepts for the genus and family levels, while the u_{1j} represents the variable slope allowed for within-genus responses.

This statistical model was adapted from prior work by Isasa et al. (2023) and van de Pol and Wright (2009). We added family as an additional random effect to account for wider phylogenetic effects, as many of the genera tested fall within a few key families. We also allowed both intercepts and slopes to vary at the genus-level to capture any deviations in responses across genera. All continuous predictors and response variables were log-transformed to satisfy normality assumptions.

The output of the model includes two R^2 values, the marginal and conditional R^2. The marginal R^2 is the proportion of the variance of vessel sizes accounted for by MAP (the fixed effect) alone. The conditional R^2 is the variance accounted for by both MAP and the taxonomic groupings (the fixed effect + all random effects). A large difference between the marginal and conditional R^2 would indicate that taxonomic grouping accounts for a significant fraction of the overall variation in data.

Variance partitioning using the performance R package reveals the contribution of the differences in intercept and slope within taxonomic groups to the total overall variance, which is possible from the decoupling of effects by levels. For example, a relationship could be weak overall because the slopes may vary greatly across genera, but there could be very consistent slopes across families.

To quantify the difference in responses between the new and traditional pooled approaches, we compared this genus-level centering model to a conventional simple linear regression of log-transformed both D_h and VLF against log-transformed MAP with no random effects (Equation 5):

306 $$y_i = \beta_0 + \beta_{\text{pooled}} x_i + \varepsilon_i. \quad (5)$$

307 This equation has only one response, with slope b_{pooled} and intercept b_0. Model
308 performance was assessed using Akaike Information Criterion (AIC) and the
309 coefficients of determination R^2 alongside slope coefficients.

310

Results

We analysed images for 480 species representing 129 genera and 32 families of Australian native species. The most diverse family, Myrtaceae (n = 221), also contained the largest genus of the study, *Eucalyptus* (n = 131). The mean hydraulically weighted diameters (D_h) ranged from 12.98 to 123.80 mm, while vessel lumen fraction (VLF) ranged from 3.13% to 31.86%. The measurements fell within the expected ranges based on a global wood anatomy database (Zanne *et al.*, 2010) (Figure S2).

Relationship of D_h with rainfall

The linear mixed-effects model with genus-level centering revealed that vessel size scales predictably with rainfall at both within- and across-genus levels (Fig. 4a). The across-genus effect (variation in mean D_h across genera) was highly significant (b_{across} = 0.37, SE = 0.11, 95% CI [0.15, 0.59], $P < 0.001$). The within-genus effect (variation among species within a genus) was equally significant and nearly identical in magnitude (b_{within} = 0.33, SE = 0.09, 95% CI [0.16, 0.51], $P < 0.001$). The precipitation variables explained 11.0% of the observed variance in D_h (marginal R^2 = 0.110), while the inclusion of genus- and family-level grouping effects increased explained variance to 78.6% (conditional R^2 = 0.786).

The simple linear regression of D_h against MAP resulted in a shallower slope (b_{pooled} = 0.16, SE = 0.04, 95% CI [0.08, 0.25], $P < 0.001$) and explained only 2.8% of the variance (R^2 = 0.028, Fig. 4). It also had a much higher AIC value (AIC = 582.5) compared to the model with genus-level centering (AIC = 193.1) which indicates a much poorer fit to the data.

VLF relationship with rainfall

VLF showed no significant relationship with rainfall at either genus or family level (Fig. 4b). The across-genus effect was non-significant (b_{across} = -0.003, SE = 0.09, 95% CI [-0.18, 0.17], P = 0.972) as well as the within-genus effect (b_{within} = 0.11, SE = 0.11, 95% CI [-0.10, 0.32], P = 0.303). The mixed-effects model explained only 0.7% of the variance of VLF with MAP (marginal R^2 = 0.007), but including the taxonomic grouping accounted for 45.6% (conditional R^2 = 0.456). The simple linear regression for this trait was also worse (AIC = 458.2 vs AIC = 369.2), and non-significant (b_{pooled} = 0.06, SE = 0.04, 95% CI [-0.01, 0.14], P = 0.110, R^2 = 0.005).

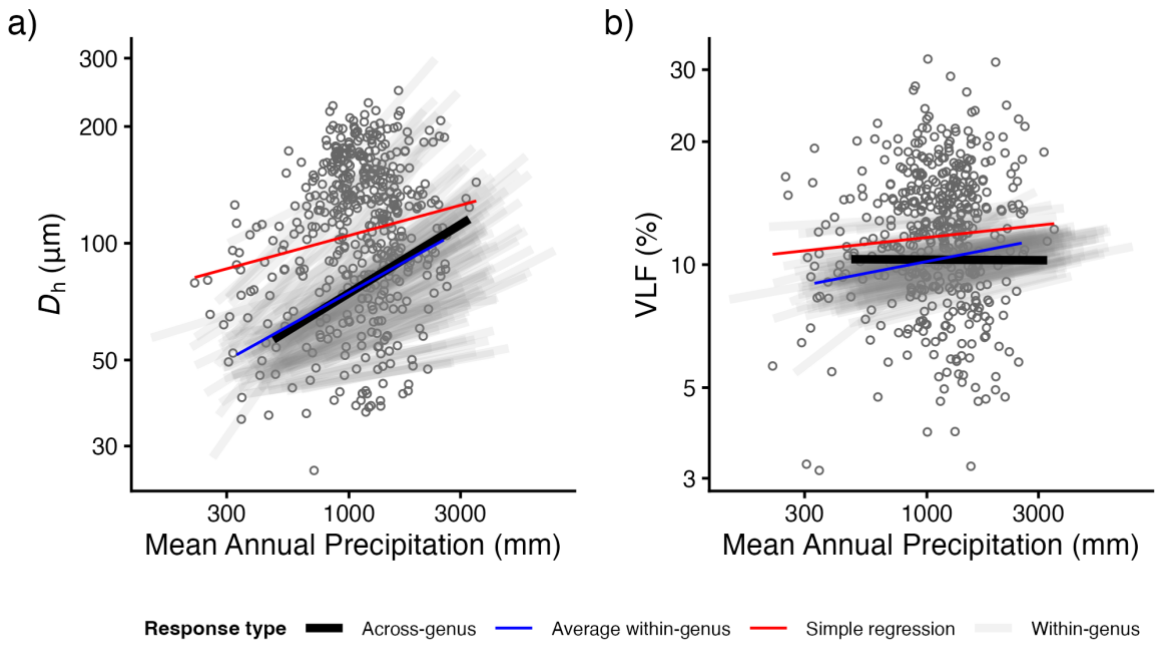

Fig. 4 The overall relationship of hydraulically weighted vessel diameter (D_h) and vessel lumen fraction (VLF) to rainfall (n = 480). The across-genus response corresponds with the average within-genus response, both of which differ in slope and intercept to the simple linear regression. The individual within-genus responses show markedly consistent slopes, mainly differing in intercepts.

Variance partitioning

The analysis of random effect variance revealed the significant influence of phylogenetic groupings on the overall variance seen for both traits (Table 2). For D_h, the differences in intercepts across genera accounted for the largest proportion of the random effect variance (SD = 0.323), with family intercepts (SD = 0.214), and genus-level slopes (SD = 0.313) also being major contributors. Similar results were found with VLF, with the differences in intercept across genera and families being significant contributors (SD = 0.169 and 0.222, respectively). However, the residual variance was much higher (SD = 0.314).

Table 2 Sources of variance from the within-genus level centering model.

	SD (s)	Variance (s^2)	% of total variance
***D*h**			
Genus (slope)	0.313	0.098	32.8%
Genus (intercept)	0.323	0.104	35.0%
Family (intercept)	0.214	0.046	15.3%
Residual	0.225	0.051	16.9%
VLF			
Genus (slope)	0.186	0.035	16.4%
Genus (intercept)	0.169	0.028	13.5%
Family (intercept)	0.222	0.049	23.4%
Residual	0.314	0.099	46.7%

Within-group responses

For genera with ten or more species, it was evident that the responses of D_h to rainfall were consistently positive, with similar slopes (Fig. 5a). The differences across genera

362 emerged mainly from the difference in intercepts. For example, *Eucalyptus*, *Corymbia*,
363 and *Flindersia* clearly diverged from both the across-genera response and the family
364 (Myrtaceae) random effect in intercept but had very similar slopes. It was also evident
365 that Fabaceae was skewed towards *Acacia* due to the sampling disproportionately
366 favouring *Acacia* species. The responses for VLF across rainfall were also consistent,
367 with some exceptions. Unlike D_h, some genera had noticeably different slopes
368 compared to the across-genera response. Specifically, *Flindersia* and *Melaleuca* had
369 notably more positive slopes compared to all the other genera (Fig. 6a).

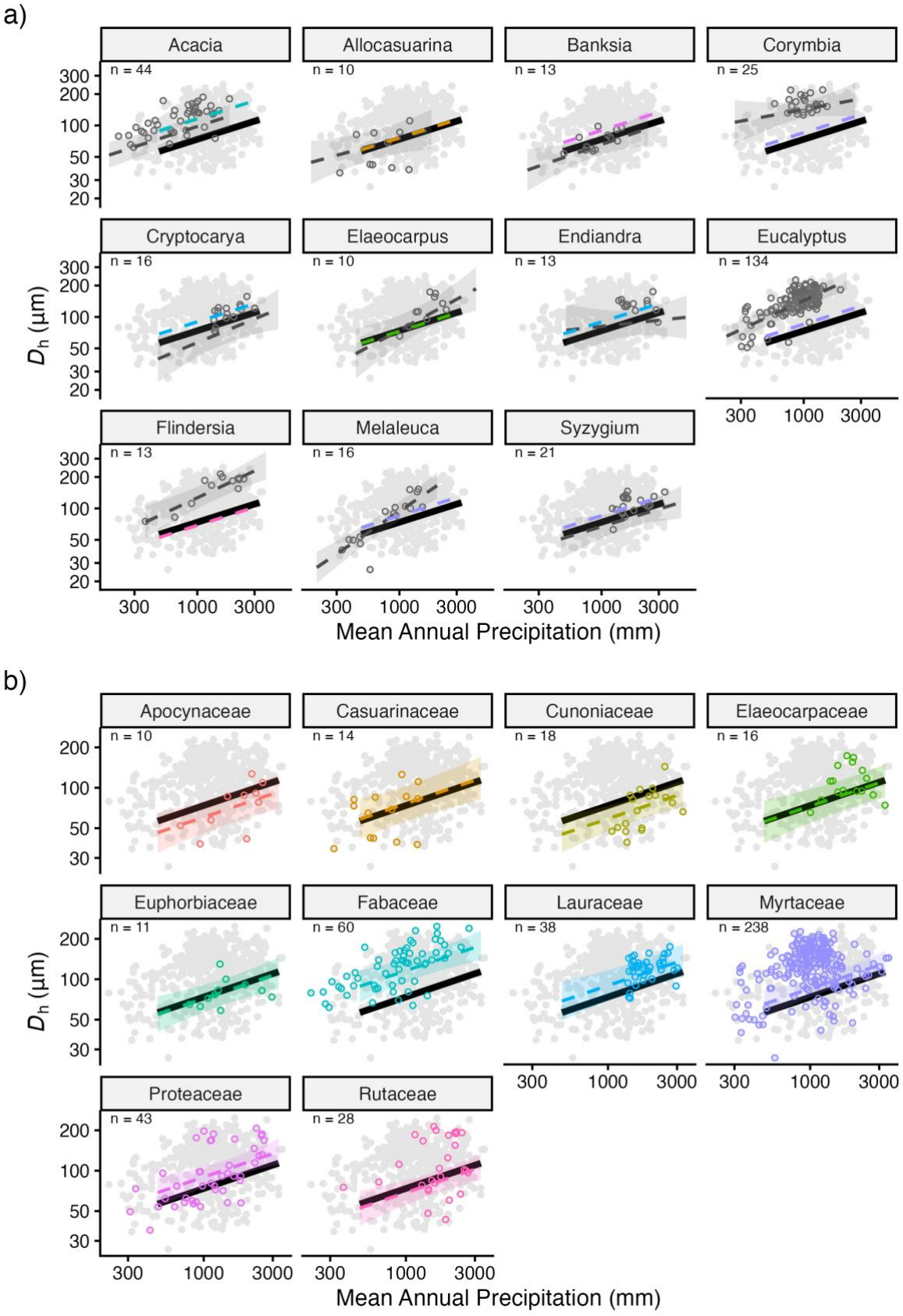

Fig. 5 Deviation in (a) within-genus responses (dashed grey lines) and (b) within-family (coloured dashed lines) of D_h to MAP against the overall across-genus response (black line). The dashed lines and points are coloured by family across both plots. Light grey dots in the background represent all 480 species.

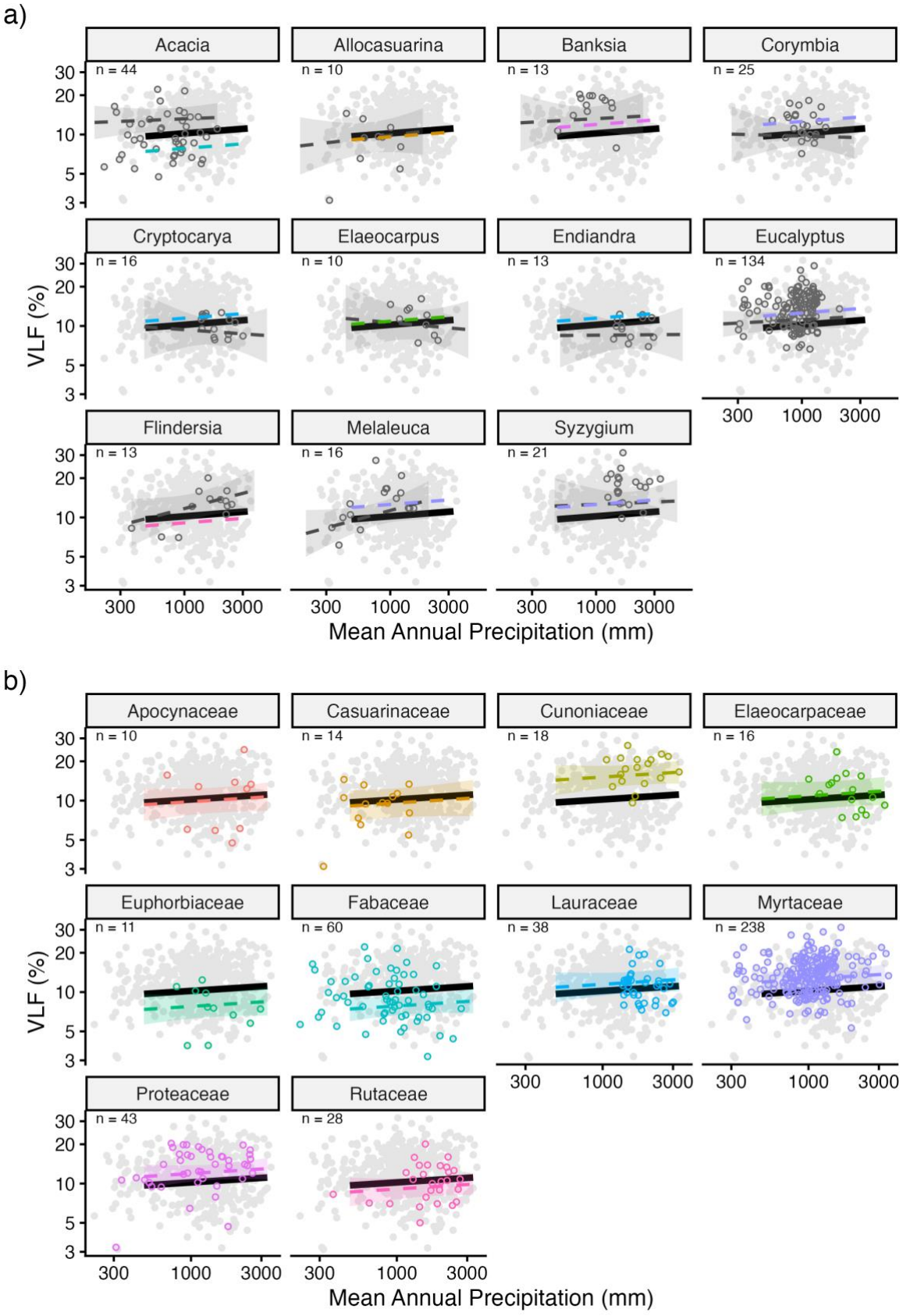

Fig. 6 Deviation in (a) within-genus responses (dashed grey lines) and (b) within-family (coloured dashed lines) of VLF to MAP against the overall across-genus response (black line). The dashed lines and points are coloured by family across both plots. Light grey dots in the background represent all 480 species.

Discussion

By explicitly partitioning within- and across-genus responses to mean annual precipitation, our results demonstrate that hydraulically weighted diameter (D_h) varies consistently with rainfall across diverse lineages, offers a promising explanation for the long-standing inconsistencies in macroecological trait-climate relationships. Here, we synthesise these findings with theoretical expectations of hydraulic trade-offs and anatomical coordination, examine the distinct evolutionary behaviour of vessel lumen fraction (VLF), and evaluate how phylogenetic structure, plant height, and analytical choices shape trait-environment scaling. Together, these sections clarify how lineage-specific architectural baselines obscure functional responses in pooled datasets and highlight the utility of hierarchical modelling for advancing large-scale plant hydraulics research.

Consistent rainfall scaling of D_h across hierarchical levels

Separating the within- and across-genus responses reveals a consistent, positive scaling of hydraulically weighted diameter with rainfall, resolving long-standing inconsistencies in macroecological studies. Our within-genus centering model, adapted from van de Pol and Wright (2009) and Isasa et al. (2023), demonstrated that D_h scales predictably with rainfall at both hierarchical levels, with highly conserved slope magnitudes (Fig. 4a) that strongly support our hypothesis that vessel size increases in wetter environments. By explicitly partitioning trait-climate relationships, our model explained 78.6% of the total variance in D_h compared to only 2.8% for a conventional pooled regression, suggesting that taxonomic (and likely phylogenetic) structure accounts for the majority of observed variance. In contrast, VLF showed no

significant relationship with rainfall at either the genus or family level, with variation primarily driven by phylogenetic grouping (Fig. 4b). This divergence in climate responsiveness mirrors findings from taxonomically restricted studies: whereas broad compilations often report weak vessel-rainfall links (Cornwell & Ackerly, 2009; Morris *et al.*, 2018; Peters *et al.*, 2021), single-genus analyses consistently reveal stronger, more predictable responses (Pfautsch *et al.*, 2016; Bourne *et al.*, 2017). Our results demonstrate that these seemingly conflicting outcomes arise from conflating within-lineage scaling with across-lineage baseline differences. These patterns closely align with the hydraulic safety-efficiency trade-off, yet their obscuration in pooled datasets highlights how phylogenetic structure can mask otherwise predictable trait-climate relationships.

Lineage-specific anatomical contexts shift baseline hydraulic strategies

The decoupling of within- and across genus effects clarifies why vessel size-rainfall relationships appear weak in broad comparative studies but emerge strongly in taxonomically restricted samples. Theory predicts that wetter environments should favour higher xylem conductivity through larger vessels (Tyree & Ewers, 1991). Our results support this expectation but reveal that evolutionary lineages embed vessels within distinct anatomical contexts that shift their baseline conductivity independent of climate. Where a lineage has evolved a distinct anatomical strategy such as dense wood, pronounced vessel grouping, or high parenchyma investment, these traits interact with rainfall-driven vessel scaling to shift baseline conductivity independently of climate (Li *et al.*, 2018). Consequently, genera like *Eucalyptus* and *Flindersia* maintain significantly higher baseline vessel sizes across their climatic ranges while

preserving the same rainfall response slope as other lineages. As Stearns (1992) argued, traits adapt to climate but also to one another, meaning the same selective pressure can yield different anatomical solutions across evolutionary groups. This multivariate trait coordination likely explains why pooled macroecological datasets often dilute climate signals and why isolating within-group variation consistently recovers stronger patterns. Recognising that trait-climate scaling operates within phylogenetically bounded architectural contexts necessitates statistical approaches that explicitly partition hierarchical variation.

Hierarchical centering resolves macroecological inconsistencies and ecological fallacies

Within-subject centering offers a robust statistical framework for macroecological studies, mitigating the ecological fallacy that arises from pooling phylogenetically diverse data. Standard linear models often conflate inter-group differences in mean trait values with within-group responses to environmental gradients, which can obscure functional patterns and lead to ecologically misleading conclusions (van de Pol & Wright, 2009). By explicitly separating the across-genus mean from within-genus deviations, our approach partitions intercept divergence from slope consistency, preserving high-resolution functional signals without collapsing taxa into taxonomic-level averages. This method proves superior to conducting separate regressions per genus, which sacrifices broader ecological context and struggles with uneven sample sizes, or to averaging traits at higher taxonomic levels, which discards intrageneric variation entirely. This model's ability to decouple hierarchical effects also aligns with the principle that plant traits are functionally coordinated rather than evolutionarily independent, making it highly transferable to other multivariate trait systems such as

449 wood density, leaf economics, or hydraulic conductivity. A similar finding was seen
450 when we applied the same model to data from Liu et al. (2019), where the relationship
451 between vessel diameter and MAP was significantly strengthened compared to
452 conventional linear models. Nevertheless, this approach is not without trade-offs: we
453 used genus-level taxonomy as a proxy for the conserved hydraulic architecture within
454 evolutionary lineages, which may not perfectly capture evolutionary divergence (Wang
455 *et al.*, 2025). Yet, despite these constraints, the framework successfully isolates
456 climate-driven scaling from lineage-specific architectural baselines. While this
457 methodological refinement clarifies vessel diameter responses, it also underscores
458 why anatomically derived proxies like VLF behave differently under the same
459 framework.

460 ## VLF reflects structural trade-offs rather than climate response

461 The absence of a rainfall signal for VLF reflects its derived nature and the tight trade-
462 offs between conducting tissue and structural functions in xylem. Unlike vessel
463 diameter, which dominates hydraulic efficiency through disproportionate scaling
464 according to the Hagen-Poiseuille law, VLF contributes to conductivity at a much lower
465 incremental rate (Zanne *et al.*, 2010). Increasing the proportion of lumen space
466 inevitably requires sacrificing non-lumen tissues such as fibre tracheid and axial
467 parenchyma, which compromises mechanical stability in tall stems and reduces the
468 plants' capacity for embolism recovery (Tyree & Zimmermann, 2002; Morris *et al.*,
469 2018). Consequently, VLF behaves more as a phylogenetically conserved trait than a
470 climate-responsive one. This pattern suggests that VLF is primarily constrained by
471 lineage-specific architectural investments rather than direct moisture-driven selection,
472 likely relating to the notable differences in wood anatomy across taxa (Fig. 2). Rather

than serving as a reliable macroecological proxy for drought resistance or vessel connectivity, VLF may be better understood alongside more direct functional indices such as vessel grouping index or parenchyma to tissue ratios, which capture connectivity and safety trade-offs more sensitively (Levionnois *et al.*, 2021). These anatomical constraints likely interact with other size-related factors, such as plant height, which have long been proposed as hidden drivers of vessel size variation.

Plant height, ontogeny, and multivariate trait coordination

The relationship between vessel size and climate is likely influenced by plant height, ontogenetic changes in stem diameter, and broader trait coordination. A prominent debate in plant hydraulics centres on whether vessel diameter scales primarily with climate or simply tracks plant height, as vessels naturally widen toward the stem base in taller individuals (Olson *et al.*, 2014; Fajardo *et al.*, 2020). Since plant height itself is strongly correlated with moisture availability on broad scales (Moles *et al.*, 2009), height and rainfall can act as colinear drivers of xylem anatomy. Although we did not explicitly model individual tree height, our genus- and family-level random intercepts likely capture lineage specific maximum heights and developmental trajectories, filtering out height-mediated vascular widening from climate-driven scaling. This aligns with studies that find strong rainfall signals when phylogenetic or architectural context is controlled (Pfautsch *et al.*, 2016), while reconciling those that attribute vessel size variation primarily to stature (Morris *et al.*, 2018; Fajardo *et al.*, 2020). Beyond height, vessel anatomy does not evolve in isolation; it is continuously buffered or amplified by coordinated traits such as wood density, axial parenchyma positioning, and vessel grouping (Zanne *et al.*, 2010; Choat *et al.*, 2018). These architectural feedbacks explain why baseline vessel sizes diverge across clades while preserving a conserved

directional response to precipitation. Consequently, treating vessel diameter as an isolated climate proxy risks misattributing phylogenetically fixed architectural constraints to environmental plasticity. While our dataset and Australian context strengthen these inferences, several methodological and geographical limitations should be considered when extrapolating these patterns.

Sampling constraints, regional context, and future directions

Our conclusions are shaped by the nature of the dataset and the ecological context of the study region. The sample is heavily weighted toward fast-growing canopy species favoured in forestry, particularly *Eucalyptus* and *Acacia*, which together make up nearly 60% of the diversity. While this reflects the structure of Australian forests (ABARES, 2023), it may underrepresent slower growing or understory lineages with distinct hydraulic strategies. Climate data were derived from species-level GBIF occurrences paired with coarse-resolution WorldClim rasters, which lack microhabitat precision and assume range-wide climatic averaging. Additionally, historical wood slides lack precise georeferencing, tree age, and stem height, limiting explicit control for ontogeny and local environmental variation. Ecologically, Australian woody vegetation is largely frost-free, so drought rather than cold likely drives hydraulic adaptation in our study system (Zanne *et al.*, 2018). This makes our findings particularly relevant for tropical and subtropical forests, though the hierarchical modelling approach remains applicable to temperate and alpine regions where drought and freezing interact. Future work should integrate molecular phylogenies, directly measure ontogenetic and architectural variables, expand into phylogenetically distinct biomes, and pair anatomical proxies with in-situ hydraulic traits like P50 and specific conductivity.

Conclusion

Our findings show that inconsistencies in vessel size-rainfall relationships largely arise from pooling taxa with different baseline hydraulic strategies. Applying genus-level centering to a phylogenetically diverse dataset reveals that hydraulically weighted vessel diameter scales predictably with precipitation when hierarchical structure is accounted for, while VLF behaves as a phylogenetically constrained trait shaped by anatomical trade-offs. Separating within- and across-group responses clarifies these patterns and offers a practical framework for future trait-climate studies. Together, these results highlight the value of historical wood collections and hierarchical modelling in linking local hydraulic function to broad biogeographical patterns.

Acknowledgements

We would like to acknowledge Hannah McPherson from the Australian Botanic Garden Mount Annan for allowing us access to the historic wood collections. This research was supported by the Commonwealth through an Australian Government Research Training Program Scholarship [DOI: https://doi.org/10.82133/C42F-K220].

Competing interests

None declared.

Author contributions

DF conceived the project. DF and JI planned the initial data curation and processing methods. JI digitised the historical wood collections. EM and ZB conducted the image processing and vessel area measurements. EM, DF, and IT conducted the data analyses and interpretation. EM wrote the manuscript, with feedback from DF and IT for the whole manuscript. JI and ZB contributed to the methods and discussion sections. AI was used for code review and suggestions for data visualisation. AI was also used to give feedback for the structure and flow of the manuscript.

Data availability

Data and data analyses code will be available when the paper is accepted by the target journal.

References

Australian Bureau of Agricultural and Resource Economics and Sciences. **2023**. Forests of Australia (2023).

Avila RT, Kane CN, Batz TA, Trabi C, Damatta FM, Jansen S, McAdam SAM. **2023**. The relative area of vessels in xylem correlates with stem embolism resistance within and between genera. *Tree Physiology* **43**: 75–87.

Bankhead P, Loughrey MB, Fernández JA, Dombrowski Y, McArt DG, Dunne PD, McQuaid S, Gray RT, Murray LJ, Coleman HG, *et al.* 2017. QuPath: Open source software for digital pathology image analysis. *Scientific Reports* **7**: 16878.

Barotto AJ, Fernandez ME, Gyenge J, Meyra A, Martinez-Meier A, Monteoliva S. **2016**. First insights into the functional role of vasicentric tracheids and parenchyma in eucalyptus species with solitary vessels: do they contribute to xylem efficiency or safety? *Tree Physiology* **36**: 1485–1497.

Bourne AE, Creek D, Peters JMR, Ellsworth DS, Choat B. **2017**. Species climate range influences hydraulic and stomatal traits in Eucalyptus species. *Annals of Botany* **120**: 123–133.

Brooks ME, Kristensen K, Benthem KJ van, Magnusson A, Berg CW, Nielsen A, Skaug HJ, Maechler M, Bolker BM. **2017**. glmmTMB Balances Speed and Flexibility Among Packages for Zero-inflated Generalized Linear Mixed Modeling. *The R Journal* **9**: 378–400.

Carlquist S. **1977**. Ecological Factors in Wood Evolution: A Floristic Approach. *American Journal of Botany* **64**: 887–896.

Choat B, Brodribb TJ, Brodersen CR, Duursma RA, López R, Medlyn BE. **2018**. Triggers of tree mortality under drought. *Nature* **558**: 531–539.

Choat B, Jansen S, Brodribb TJ, Cochard H, Delzon S, Bhaskar R, Bucci SJ, Feild TS, Gleason SM, Hacke UG, *et al.* 2012. Global convergence in the vulnerability of forests to drought. *Nature* **491**: 752–755.

Cornwell WK, Ackerly DD. **2009**. Community assembly and shifts in plant trait distributions across an environmental gradient in coastal California. *Ecological Monographs* **79**: 109–126.

Dong Y, Li Z, Keyimu M, Chen Y, Gao G, Wang C, Wang X. **2022**. A Comparative Analysis of the Hydraulic Strategies of Non-Native and Native Perennial Forbs in Arid and Semiarid Areas of China. *Forests* **13**: 193.

Fajardo A, Martinez-Perez C, Cervantes-Alcayde MA, Olson ME. **2020**. Stem length, not climate, controls vessel diameter in two trees species across a sharp precipitation gradient. *New Phytologist* **225**: 2347–2355.

Fick SE, Hijmans RJ. **2017**. WorldClim 2: new 1-km spatial resolution climate surfaces for global land areas. *International Journal of Climatology* **37**: 4302–4315.

GBIF.org User. **2026**. Occurrence Download.

Gleason SM, Butler DW, Waryszak P. **2013**. Shifts in Leaf and Stem Hydraulic Traits across Aridity Gradients in Eastern Australia. *International Journal of Plant Sciences* **174**: 1292–1301.

Gleason SM, Butler DW, Ziemińska K, Waryszak P, Westoby M. **2012**. Stem xylem conductivity is key to plant water balance across Australian angiosperm species. *Functional Ecology* **26**: 343–352.

Gleason SM, Westoby M, Jansen S, Choat B, Hacke UG, Pratt RB, Bhaskar R, Brodribb TJ, Bucci SJ, Cao KF, *et al.* 2016. Weak tradeoff between xylem safety and xylem-specific hydraulic efficiency across the world's woody plant species. *New Phytologist* **209**: 123–136.

Isasa E, Link RM, Jansen S, Tezeh FR, Kaack L, Sarmento Cabral J, Schuldt B. **2023**. Addressing controversies in the xylem embolism resistance–vessel diameter relationship. *New Phytologist* **238**: 283–296.

Levionnois S, Jansen S, Wandji RT, Beauchêne J, Ziegler C, Coste S, Stahl C, Delzon S, Authier L, Heuret P. **2021**. Linking drought-induced xylem embolism resistance to wood anatomical traits in Neotropical trees. *New Phytologist* **229**: 1453–1466.

Li XM, Blackman CJ, Choat B, Duursma RA, Rymer PD, Medlyn BE, Tissue DT. **2018**. Tree hydraulic traits are coordinated and strongly linked to climate-of-origin across a rainfall gradient. *Plant Cell and Environment* **41**: 646–660.

Liu H, Gleason SM, Hao G, Hua L, He P, Goldstein G, Ye Q. **2019**. Hydraulic traits are coordinated with maximum plant height at the global scale. *Science Advances* **5**: eaav1332.

Lüdecke D, Ben-Shachar MS, Patil I, Wiernik BM, Bacher E, Thériault R, Makowski D. **2022**. easystats: Framework for Easy Statistical Modeling, Visualization, and Reporting. *CRAN*.

Martínez-Cabrera HI, Jones CS, Espino S, Schenk HJ. **2009**. Wood anatomy and wood density in shrubs: Responses to varying aridity along transcontinental transects. *American Journal of Botany* **96**: 1388–1398.

Moles AT, Warton DI, Warman L, Swenson NG, Laffan SW, Zanne AE, Pitman A, Hemmings FA, Leishman MR. **2009**. Global patterns in plant height. *Journal of Ecology* **97**: 923–932.

Morris H, Gillingham MAF, Plavcová L, Gleason SM, Olson ME, Coomes DA, Fichtler E, Klepsch MM, Martínez-Cabrera HI, McGlinn DJ, *et al.* 2018. Vessel diameter is related to amount and spatial arrangement of axial parenchyma in woody angiosperms. *Plant, Cell & Environment* **41**: 245–260.

Morris H, Plavcová L, Cvecko P, Fichtler E, Gillingham MAF, Martínez-Cabrera HI, McGlinn DJ, Wheeler E, Zheng J, Ziemińska K, *et al.* 2016. A global analysis

of parenchyma tissue fractions in secondary xylem of seed plants. *New Phytologist* **209**: 1553–1565.

Mrad A, Johnson DM, Love DM, Domec J-C. **2021**. The roles of conduit redundancy and connectivity in xylem hydraulic functions. *New Phytologist* **231**: 996–1007.

Olson ME, Anfodillo T, Rosell JA, Petit G, Crivellaro A, Isnard S, León-Gómez C, Alvarado-Cárdenas LO, Castorena M. **2014**. Universal hydraulics of the flowering plants: vessel diameter scales with stem length across angiosperm lineages, habits and climates. *Ecology Letters* **17**: 988–997.

Peters JMR, López R, Nolf M, Hutley LB, Wardlaw T, Cernusak LA, Choat B. **2021**. Living on the edge: A continental-scale assessment of forest vulnerability to drought. *Global Change Biology* **27**: 3620–3641.

Pfautsch S, Harbusch M, Wesolowski A, Smith R, Macfarlane C, Tjoelker MG, Reich PB, Adams MA. **2016**. Climate determines vascular traits in the ecologically diverse genus Eucalyptus. *Ecology Letters* **19**: 240–248.

van de Pol M, Wright J. **2009**. A simple method for distinguishing within- versus between-subject effects using mixed models. *Animal Behaviour* **77**: 753–758.

R Core Team. **2026**. *R: A Language and Environment for Statistical Computing*. Vienna, Austria: R Foundation for Statistical Computing.

Schreiber SG, Hacke UG, Hamann A. **2015**. Variation of xylem vessel diameters across a climate gradient: insight from a reciprocal transplant experiment with a widespread boreal tree. *Functional Ecology* **29**: 1392–1401.

Sperry JS, Meinzer FC, McCulloh KA. **2008**. Safety and efficiency conflicts in hydraulic architecture: scaling from tissues to trees. *Plant, Cell & Environment* **31**: 632–645.

Sperry J, Saliendra N. **1994**. Intra-and inter-plant variation in xylem cavitation in Betula occidentalis. *Plant, Cell & Environment* **17**: 1233–1241.

Stearns SC. **1992**. The evolution of life histories.

Towers IR, O'Reilly-Nugent A, Sabot MEB, Vesk PA, Falster DS. **2024**. Optimising height-growth predicts trait responses to water availability and other environmental drivers. *Plant, Cell & Environment* **47**: 4849–4869.

Tyree MT, Ewers FW. **1991**. The hydraulic architecture of trees and other woody plants. *New Phytologist* **119**: 345–360.

Tyree M, Zimmermann M. **2002**. *Xylem Structure and The Ascent of Sap*.

Wang Y, Liesche J, Crivellaro A, Doležal J, Altman J, Chiatante D, Dimitrova A, Fan Z, Fu P, Forest F, *et al.* 2025. Physical constraints and environmental factors shape phloem anatomical traits in woody angiosperm species. *New Phytologist* **248**: 2316–2330.

Wenk EH, Cornwell WK, Fuchs A, Kar F, Monro AM, Sauquet H, Stephens RE, Falster DS. **2024**. APCalign: an R package workflow and app for aligning and updating flora names to the Australian Plant Census. *Australian Journal of Botany* **72**: BT24014.

Wickham H, Averick M, Bryan J, Chang W, McGowan LD, François R, Grolemund G, Hayes A, Henry L, Hester J, *et al.* 2019. Welcome to the Tidyverse. *Journal of Open Source Software* **4**: 1686.

Zanne AE, Pearse WD, Cornwell WK, McGlinn DJ, Wright IJ, Uyeda JC. **2018**. Functional biogeography of angiosperms: life at the extremes. *New Phytologist* **218**: 1697–1709.

Zanne AE, Tank DC, Cornwell WK, Eastman JM, Smith SA, FitzJohn RG, McGlinn DJ, O'Meara BC, Moles AT, Reich PB, *et al.* 2014. Three keys to the radiation of angiosperms into freezing environments. *Nature* **506**: 89–92.

Zanne AE, Westoby M, Falster DS, Ackerly DD, Loarie SR, Arnold SEJ, Coomes DA. **2010**. Angiosperm wood structure: Global patterns in vessel anatomy and their relation to wood density and potential conductivity. *American Journal of Botany* **97**: 207–215.

Zheng J, Zhao X, Morris H, Jansen S. **2019**. Phylogeny Best Explains Latitudinal Patterns of Xylem Tissue Fractions for Woody Angiosperm Species Across China. *Frontiers in Plant Science* **10**.

Supporting Information

Article title: Within- and across-genus scaling of vessel diameter reveals consistent hydraulic responses to rainfall

Authors: Elijah Magistrado, Isaac Towers, Jugo Ilic, Zoe Ball, Daniel Falster

The following Supporting Information is available for this article:

Fig. S1 Summary of the image processing pipeline using an *Acacia falciformis* sample.

Fig. S2 Verification of xylem vessel measurements

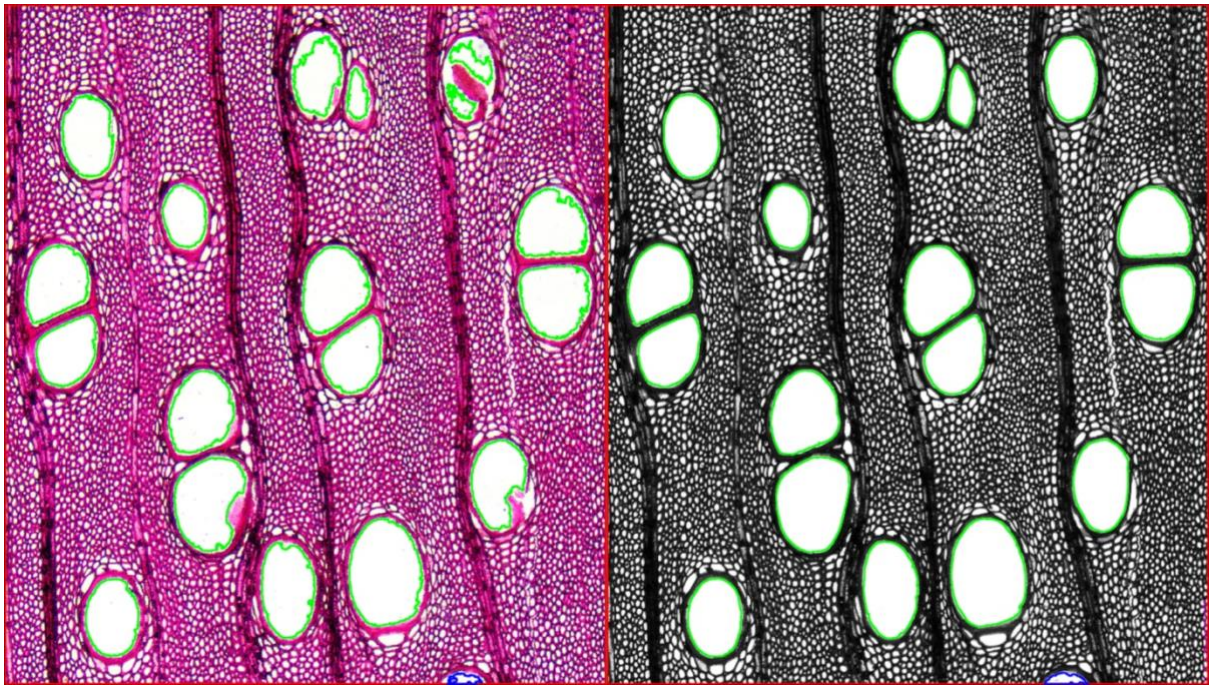

Fig. S1 Comparison of the full vessel area measurements (green lines) and part vessel measurements (blue lines) from the unmodified (left) and modified (right) images. Note the difference seen in the vessel in the top right of the images. The image is a sample of *Acacia falciformis* collected from New South Wales, Australia.

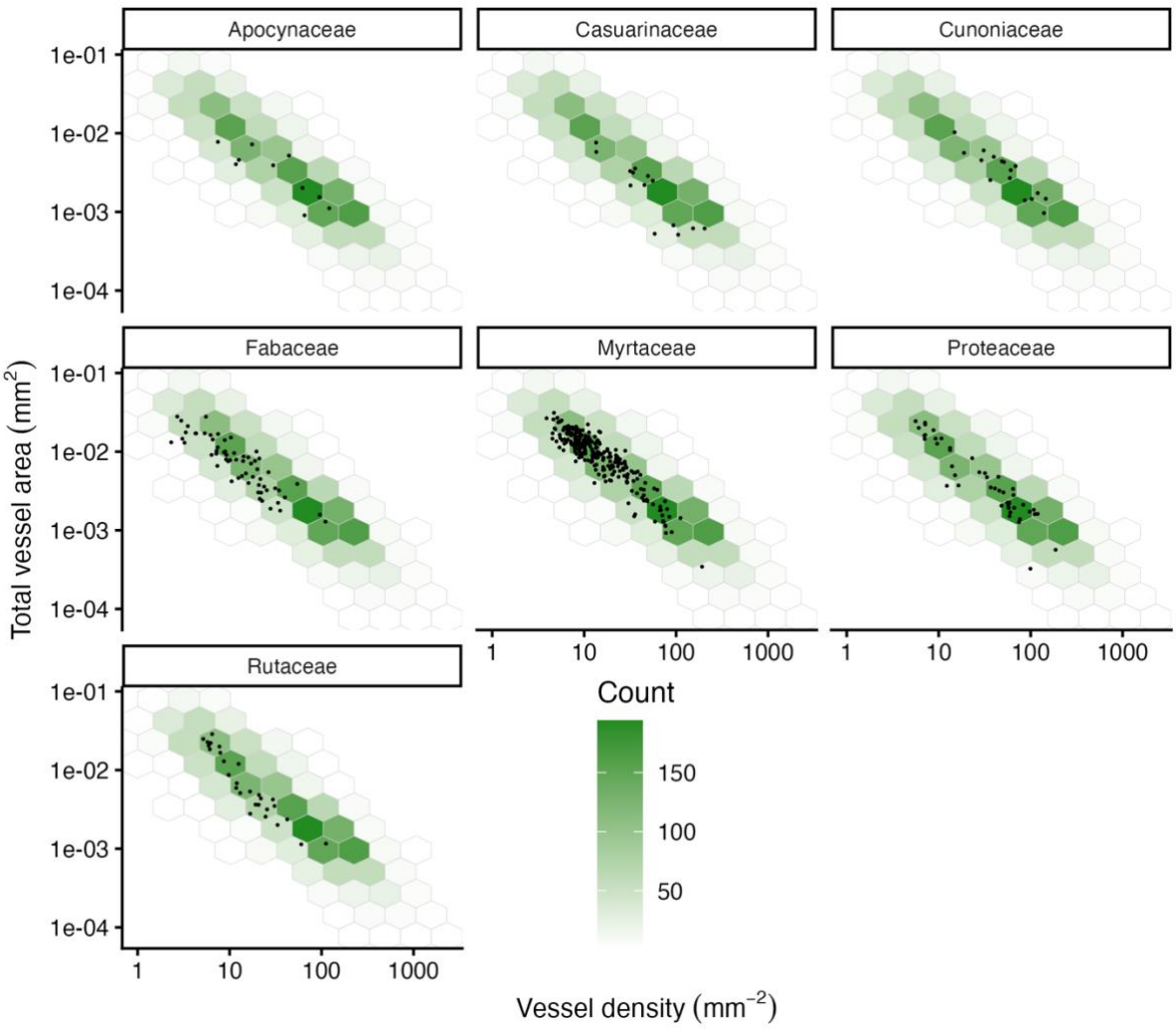

701

702 **Fig. S2** Vessel measurements are within the expected values based on a global
703 angiosperm vessel trait dataset from Zanne et al. (2010). Only families that are
704 present in both datasets are shown.